Iraqi Journal of Oil & Gas Research, Vol. 05, No. 2 (2025)

Iraqi Journal of Oil & Gas Research

Journal homepage:https://ijogr.uotechnology.edu.iq/

Mitigation of Black Powder in Gas Pipelines Using $ZnCl_2$ and $NaNO_3$: Elemental Composition Changes Monitored by XRF

[1]Anfal H. Sadeq

[1]Gas Engineering Department, College of Oil and Gas Engineering, University of Technology, Baghdad, Iraq.

Article information

Article history:
Received: September, 05, 2025
Revised: September, 27, 2025
Accepted: September, 28, 2025
Available online: October, 04, 2025

Keywords:
Natural gas pipelines,
black powder,
ZnCl2,
NaNO3,
XRF.

Corresponding Author:
Anfal H. Sadeq
150044@uotechnology.edu.iq

Abstract

With global energy demand on the rise, natural gas continues to hold a crucial role in meeting the world's energy needs. This growing reliance also brings practical challenges, one of the most important being the contamination of pipelines with black powder. Reducing these pollutants, which threaten pipeline integrity and transmission efficiency, is critical to ensure sustainable gas supplies and maintain system performance. The study aims to investigate the effect of chemical treatments with zinc chloride ($ZnCl_2$) and sodium nitrate ($NaNO_3$) on the composition of black powder taken from an Iraqi gas pipeline. Samples were treated with solutions at concentrations of 5, 7, and 10% for each component and inspected using X-ray fluorescence (XRF) to evaluate their effect. The results demonstrated that $ZnCl_2$ reduced iron oxide (Fe_2O_3) content by about 32%, while $NaNO_3$ achieved a slight reduction in Fe_2O_3. Treatment with $ZnCl_2$ successfully reduced iron content but introduced secondary contaminants, while $NaNO_3$ achieved a cleaner, though less intense, effect. This suggests that chemical treatments can significantly alter the composition of black powder and improve pipeline maintenance strategies.

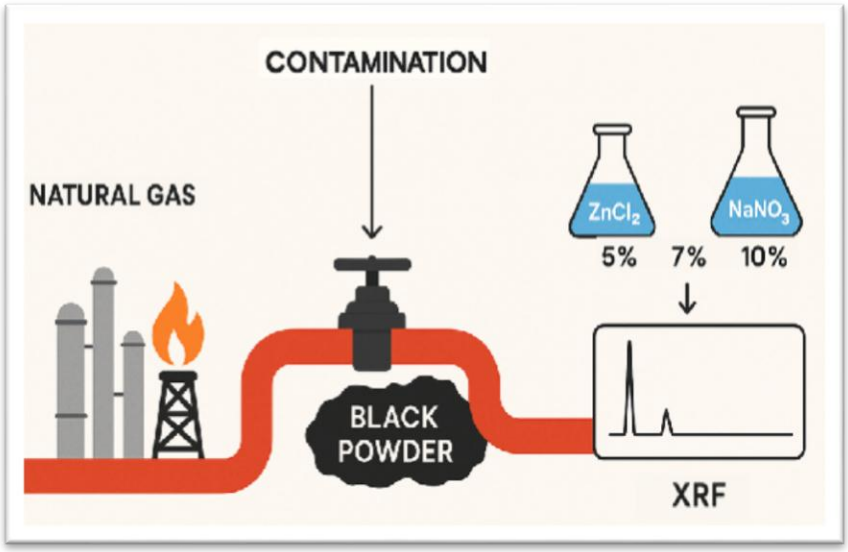

DOI: http://doi.org/10.55699/ijogr.2025.0502.1092 , College of Oil and Gas Engineering, University of Technology-Iraq

1. Introduction

By 2050, global energy demand is expected to rise sharply, especially in industrialized regions such as Asia (1). While renewable energy sources continue to expand, natural gas is expected to remain a major component of the global energy mix due to its relatively low carbon emissions compared to fossil fuels (2). As reported by the International Energy Agency (IEA), global demand for natural gas grew by about 2.5% in 2024, reaching a record level, driven largely by the power generation and industrial sectors (3). Under this scenario, the U.S. Energy Information Administration (EIA) expects that global natural gas consumption will increase by 11–57% from 2022 to 2050 (4). As countries shift to cleaner energy sources, natural gas is expected to remain a staple for electricity generation, industry, and heating (2). The continued expansion of its use is essential for maintaining and strengthening the infrastructure supporting its production, transmission, and distribution (5). Black powder buildup is one of the recurring problems faced in natural gas pipelines. It is a fine, abrasive material that mostly contains iron oxides and iron sulfides, but it also carries other particles such as dust and sand. The deposits are mainly the result of internal corrosion, where the pipe wall reacts with hydrocarbons or with corrosive gases like carbon dioxide and hydrogen sulfide. Once produced, the powder does not remain in place; it moves through the system, raising pressure drops and wearing down components such as valves, filters, compressors, and meters. In practice, this leads to poorer gas quality, higher maintenance costs, reduced efficiency, and in some cases safety risks as well (6). Much of the research so far has looked at understanding what black powder is made of and how it affects operations. Only a smaller number of studies have focused on what to do once it has already formed. Early work emphasized its link to corrosion products, especially sulfides and oxides of iron. Others tried to address the problem by physical removal methods like pigging and filtration. These helped to some extent, but they often failed when dealing with very fine or magnetically neutral particles (7–9). Later, attention shifted toward the use of chemical inhibitors to slow or prevent internal corrosion. During the late 2000s and early 2010s, amine- and phosphate-based inhibitors were tested for this purpose (10). More recently, Al Wahedi and colleagues (2020) suggested a broader approach that combines adsorption, moisture removal, and magnetic separation to reduce black powder in circulating gas systems (11). In a separate study, Debouza et al. (2020) presented a practical method for estimating black powder concentrations in pipe networks using a look-up table model, confirming the importance of observing pollutant distribution to ensure effective maintenance (12). Taken together, previous studies indicate that a mix of chemical, physical, and monitoring strategies can improve the handling of black powder. However, very little work has been focused on the direct chemical treatment of black powder once it has been collected. To address this gap, the present study examines the use of zinc chloride ($ZnCl_2$) and sodium nitrate ($NaNO_3$) at concentrations of 5%, 7%, and 10%, and evaluates their effects on elemental composition through X-ray fluorescence (XRF). The intention is to offer clearer insight into how chemical treatments might serve as a complementary tool for managing pipeline contaminants.

2. Method

2.1 Materials Used

Black powder samples were collected with the help of the Iraqi Petroleum Pipelines Company. In this case, the material was taken from the Iraqi–Iranian natural gas transmission line, where deposits had built up during operation. For the chemical tests, we worked with zinc chloride ($ZnCl_2$) and sodium nitrate ($NaNO_3$). Both chemicals were supplied in a purity grade of about 99%. The chemicals were purchased from local suppliers as standard laboratory reagents and used without any additional purification.

2.2 Equipment

All chemical treatments were carried out with an ultrasonic cleaner from Camel Sonic DG450-SK-2.3L that operates at 40–100 kHz. This device ensured the uniform dispersion of black powder samples in chemical solutions. To avoid alteration of sample composition, filtered samples were dried in a drying oven at a controlled temperature of 40–50 °C. The Iraqi German Laboratory, College of Science, Department of Geology, Iraqi German Laboratory, carried out a Spectro Xepos X-ray fluorescence (XRF) spectrometer (Ametek, Germany) for the analysis of elements in both treated and untreated samples. The instrument uses energy-dispersive XRF technology to determine elemental composition in solid samples precisely. Each pellet was measured twice, and the final results are the average of those two measurements. The standard deviation was calculated to determine the error margins, which were less than ±0.5% for all major elements reported. All results are expressed as oxides (e.g., Fe_2O_3, SiO_2, Al_2O_3), except chlorine (Cl), which is reported elementally.

2.3 Experiments

To begin treatment, 4 grams of black powder were accurately weighed and transferred into a 100 mL glass beaker. A prepared solution of zinc chloride ($ZnCl_2$) or sodium nitrate ($NaNO_3$) at concentrations of 5%, 7%, or 10% was then added in a volume of 40 mL to maintain a 1:10 (w/v) solid-to-liquid ratio. For the 1:20 (w/v) ratio, 80 mL of solution per 4 grams of powder was used. At the start, the suspension was stirred gently with a glass rod so the powder would spread evenly in the solution (13, 14). The beaker was then placed in an ultrasonic bath and sonicated for no more than 5 minutes. We kept an eye on the temperature during this step, making sure it stayed below 50 °C, since higher values could have changed the sample's composition. The idea behind the ultrasonic treatment was simply to improve contact between the solution and the powder surface, so the reaction could proceed more effectively (15). After sonication, the mixture was poured through filter paper to separate the liquid from the solid. The residue on the filter was washed three times with 20 mL of deionized water to remove any salts that were left behind. At this stage, the solid was collected and left to dry in air at room temperature. To finish, it was placed in a drying oven at 40–50 °C, which ensured all moisture was removed without damaging the material. At this point, the dried black powder was ground by hand and pressed into small, uniform pellets. Each pellet was stored in a labeled container. These samples were then set aside for elemental analysis, where they could be compared directly with the untreated material.

Figure 1: Initial appearance of black powder–solution mixture before ultrasonic treatment.

Figure 2: Sample inside ultrasonic for particle dispersion (5 min treatment, controlled temperature).

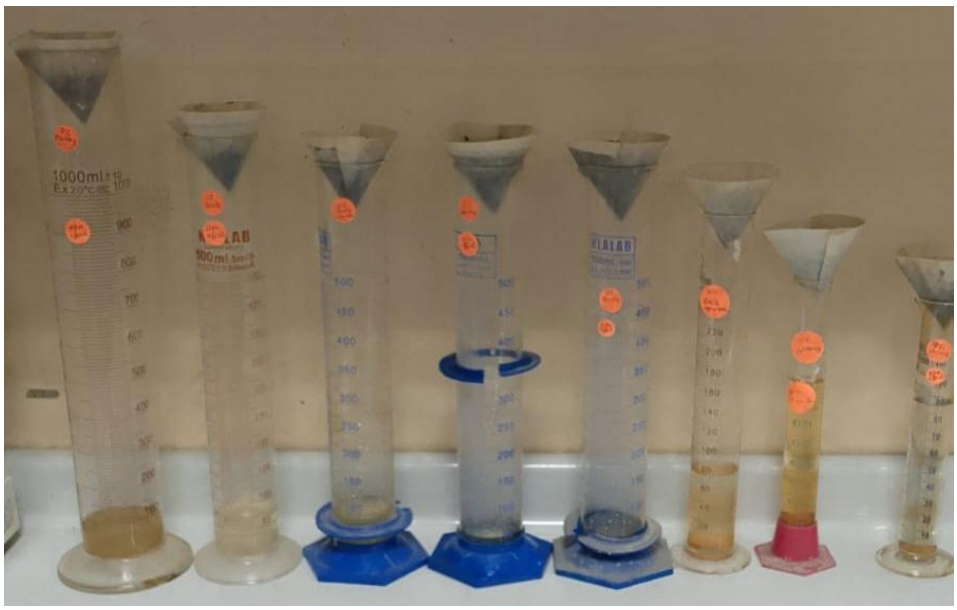

Figure 3: Samples undergoing the filtration process

.

Table 1: Summary of Chemical Solution Preparation and Experimental Conditions

Chemical	Concentration (wt%)	Preparation Formula (per 100 mL)	Treatment Ratios (solid: solution, w/v)
Zinc Chloride ($ZnCl_2$)	5%	5 g $ZnCl_2$ + 95 mL distilled water	1:10 (4 g: 40 mL) 1:20 (4 g: 80 mL)
	7%	7 g $ZnCl_2$ + 93 mL distilled water	
	10%	10 g $ZnCl_2$ + 90 mL distilled water	
Sodium Nitrate ($NaNO_3$)	5%	5 g $NaNO_3$ + 95 mL distilled water	1:10 (4 g: 40 mL) 1:20 (4 g: 80 mL)
	7%	7 g $NaNO_3$ + 93 mL distilled water	
	10%	10 g $NaNO_3$ + 90 mL distilled water	

3. Results and Discussion

3.1. Composition of Untreated Black Powder

X-ray fluorescence (XRF) analysis of the untreated black powder sample collected from an Iraqi–Iranian natural gas transmission pipeline revealed a complex mixture of corrosion products and environmental particulates. The analysis revealed that iron oxide (Fe_2O_3) was the predominant compound, making up about 59 wt% of the overall composition. This result points to oxidized iron as the primary reason for black powder formation. A smaller but notable amount of sulfur trioxide (SO_3, ~0.15 wt%) was also detected. In this case, the signal is often linked to hydrogen sulfide (H_2S) in the gas stream, which suggests that sulfide-related corrosion is present (16, 17). A very small amount of chlorine (Cl, ~0.01 wt%) was also found. Such traces are usually tied to localized chloride corrosion and may come from leftover salts or other small impurities in the pipeline (18). Beyond these, several oxides appeared in noticeable amounts: silicon dioxide (SiO_2, ~10.4 wt%), calcium oxide (CaO, ~6.2 wt%), magnesium oxide (MgO, ~3.5 wt%), and aluminum oxide (Al_2O_3, ~3.0 wt%). These compounds are most likely introduced from external sources such as dust, sand, scaling products, or other contaminants, all of which add to the abrasive and fouling behavior of black powder (19). Altogether, the identified oxides accounted for roughly 85.5 wt%. The remainder was attributed to loss of ignition (LOI), which includes bound water, carbonates, volatile organics, and trace elements not detectable by XRF.

3.2. Impact of $ZnCl_2$ Treatment

The elemental composition of black powder samples treated with $ZnCl_2$ solutions at different concentrations (5%, 7%, and 10%) and dilution ratios (1:10 and 1:20 w/v) was assessed by X-ray fluorescence (XRF). The results are summarized in Table 2 and Figure 4. The main oxides identified were iron oxide (Fe_2O_3), zinc oxide (ZnO), chlorine (Cl), silicon dioxide (SiO_2), aluminum oxide (Al_2O_3), calcium oxide (CaO), and magnesium oxide (MgO). A drop in Fe_2O_3 was clear after treatment, going from 59.0 wt% in the untreated sample to around 40.2 wt% at the lowest point. In this case, the reduction seems to come from dissolution together with chloride complexation. Under chloride-rich acidic conditions, Fe_2O_3 surfaces can be protonated and form chloride complexes such as $[FeCl_4]^-$, which makes the oxide more soluble and easier to leach out (20). Ultrasonic agitation played a role as well, since it improves mass transfer and helps break up surface oxide layers (21). Meanwhile, ZnO showed a sharp rise—from just ~0.01 wt% in the untreated sample to between 9.6 and 16.8 wt% after treatment. This increase fits with the hydrolysis of $ZnCl_2$ in solution, forming $Zn(OH)_2$, which then dehydrates to ZnO as the samples dry (22, 23). As expected, the higher the $ZnCl_2$ concentration, the more ZnO was found, which supports this pathway. SiO_2 stayed pretty stable at 10.2–10.9 wt%, consistent with its inert behavior under mild acidic conditions. Al_2O_3, in contrast, rose from ~3.0 wt% to 6.1–6.4 wt%. This apparent enrichment may be due to the loss of Fe_2O_3 making Al_2O_3 relatively higher, or possibly from the precipitation of insoluble aluminum hydroxides. CaO decreased from 6.2 wt% to 3.6–3.9 wt%, suggesting partial dissolution. Even so, some CaO likely persisted as stable phases such as calcium silicates or aluminates, which are less reactive than $ZnCl_2$ (23, 25). Small declines were also seen in MgO, Na_2O, and K_2O. These oxides are usually more soluble in aqueous systems, so partial leaching is expected, although some portions probably remained bound in more stable phases (26, 27). Trace components such as MnO, P_2O_5, and SO_3 exhibited minor changes, which may be attributed to adsorption–desorption dynamics, redox transformations (particularly for Mn), or the precipitation and dissolution of soluble phases during wet–dry cycling and CO_2 exposure (28).

Table 2: Composition of black powder samples treated with $ZnCl_2$ solutions at different concentrations.

Oxide	Treatment condition						
	Untreated	10% – 1:10	10% – 1:20	7% – 1:10	7% – 1:20	5% – 1:10	5% – 1:20
Fe_2O_3	59.00	42.00	40.20	43.20	42.10	44.00	43.10
ZnO	0.01	15.00	16.80	11.80	13.00	9.60	10.50
Cl	0.01	8.00	8.60	6.40	6.90	5.10	5.60
SiO_2	10.40	10.50	10.20	10.70	10.60	10.90	10.80
Al_2O_3	3.00	6.20	6.10	6.30	6.20	6.40	6.30
CaO	6.20	3.80	3.90	3.70	3.80	3.60	3.70
MgO	3.50	3.40	3.30	3.45	3.35	3.48	3.42
Na_2O	0.40	0.35	0.33	0.37	0.36	0.34	0.35
K_2O	1.40	1.20	1.15	1.25	1.18	1.22	1.20
TiO_2	0.90	0.85	0.82	0.87	0.84	0.86	0.85
MnO	0.10	0.12	0.11	0.13	0.12	0.11	0.12
P_2O_5	0.20	0.21	0.20	0.22	0.21	0.20	0.21
SO_3	0.15	0.20	0.22	0.18	0.19	0.17	0.18
BaO	0.10	0.11	0.10	0.12	0.11	0.10	0.11
Others	0.13	0.14	0.15	0.15	0.14	0.15	0.14

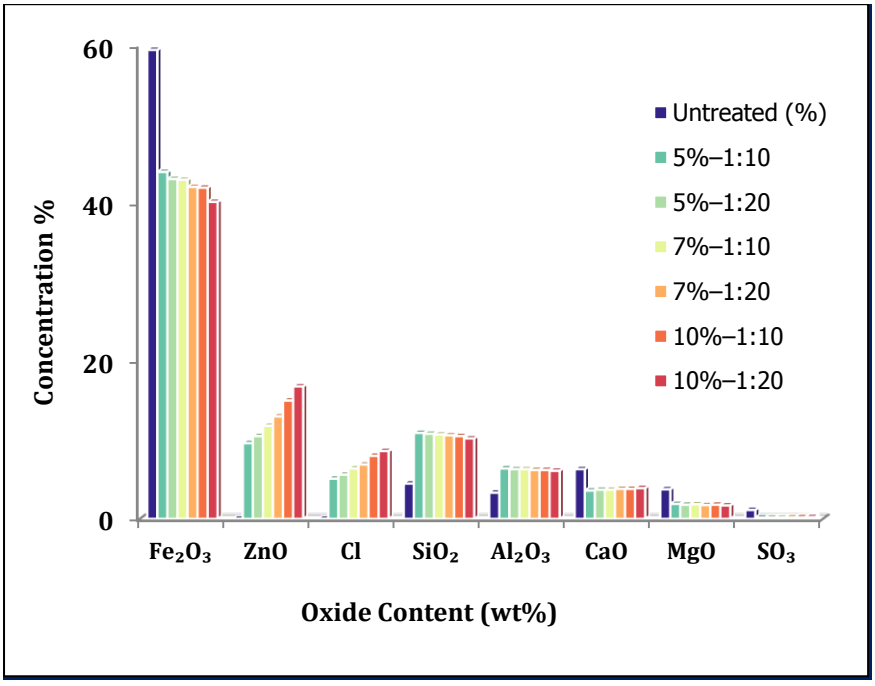

Figure 4: Effect of $ZnCl_2$ treatment on black powder composition.

3.3. Impact of $NaNO_3$ Treatment

The elemental composition of black powder samples treated with varying concentrations of $NaNO_3$ solutions (5%, 7%, and 10%) at two dilution ratios (1:10 and 1:20 w/v) was analyzed using X-ray fluorescence (XRF), as shown in Table 3 and Figure 5. Principal oxides identified include iron oxide (Fe_2O_3), sodium oxide (Na_2O), silicon dioxide (SiO_2), aluminum oxide (Al_2O_3), calcium oxide (CaO), and magnesium oxide (MgO), along with minor components such as sulfur trioxide (SO_3), phosphorus pentoxide (P_2O_5), and manganese oxide (MnO). When the black powder was treated with $NaNO_3$, the Fe_2O_3 content dropped from roughly 59 wt% in the untreated sample to between 48.5 and 54 wt%. This change appears to stem from the oxidative action of nitrate ions (NO_3^-). In such conditions, iron oxides can undergo partial dissolution through redox reactions, where Fe^{2+} is oxidized to Fe^{3+} and soluble nitrate complexes form (29). The use of ultrasonic agitation probably amplified

this effect by shaking loose surface layers and improving the transfer of iron-rich particles into solution (21). Sodium oxide (Na_2O) showed a clear increase, rising from about 0.40 wt% in the untreated sample to 1.3–1.8 wt% under the 10%/1:20 condition. This suggests that sodium from the treatment medium was retained, with Na^+ ions attached to particle surfaces or embedding within surface films during drying. Sulfur trioxide (SO_3) declined from ~0.15 wt% to 0.09–0.12 wt%. The stronger the $NaNO_3$ concentration, the larger the drop, which supports the idea that nitrate contributes to the oxidation of sulfur species into soluble or volatile forms during treatment. Other oxides—including SiO_2, Al_2O_3, and CaO—remained largely stable, showing only minor fluctuations. Their persistence highlights their resistance to leaching under these conditions (25, 24). Slight shifts were also recorded in MgO, K_2O, TiO_2, and a few trace oxides (MnO, P_2O_5, BaO). By contrast, ZnO and Cl stayed negligible (~0.01 wt%), confirming that the $NaNO_3$ treatment did not introduce zinc or chloride. Taken together, the data show that $NaNO_3$ mainly affects iron and sulfur species while leaving most other oxides intact.

Table 3: Composition of black powder samples treated with $NaNO_3$ solutions at different concentrations

Oxide	Treatment condition						
	Untreated	10%–1:10	10%–1:20	7%–1:10	7%–1:20	5%–1:10	5%–1:20
Fe_2O_3	59.00	50.00	48.50	52.00	51.00	54.00	52.50
ZnO	0.01	0.01	0.01	0.01	0.01	0.01	0.01
Cl	0.01	0.01	0.01	0.01	0.01	0.01	0.01
SiO_2	10.40	10.40	10.50	10.40	10.40	10.30	10.40
Al_2O_3	3.00	3.05	3.00	3.10	3.05	3.00	3.05
CaO	6.20	6.20	6.15	6.25	6.20	6.15	6.20
MgO	3.50	3.45	3.50	3.40	3.45	3.50	3.45
Na_2O	0.40	1.50	1.80	1.30	1.60	1.20	1.40
K_2O	1.40	1.35	1.38	1.32	1.35	1.38	1.35
TiO_2	0.90	0.88	0.89	0.90	0.88	0.89	0.88
MnO	0.10	0.10	0.09	0.10	0.09	0.10	0.09
P_2O_5	0.20	0.20	0.19	0.20	0.19	0.20	0.19
SO_3	0.15	0.10	0.09	0.11	0.10	0.12	0.11
BaO	0.10	0.09	0.10	0.09	0.10	0.09	0.10
Others	0.13	0.14	0.15	0.14	0.15	0.14	0.15

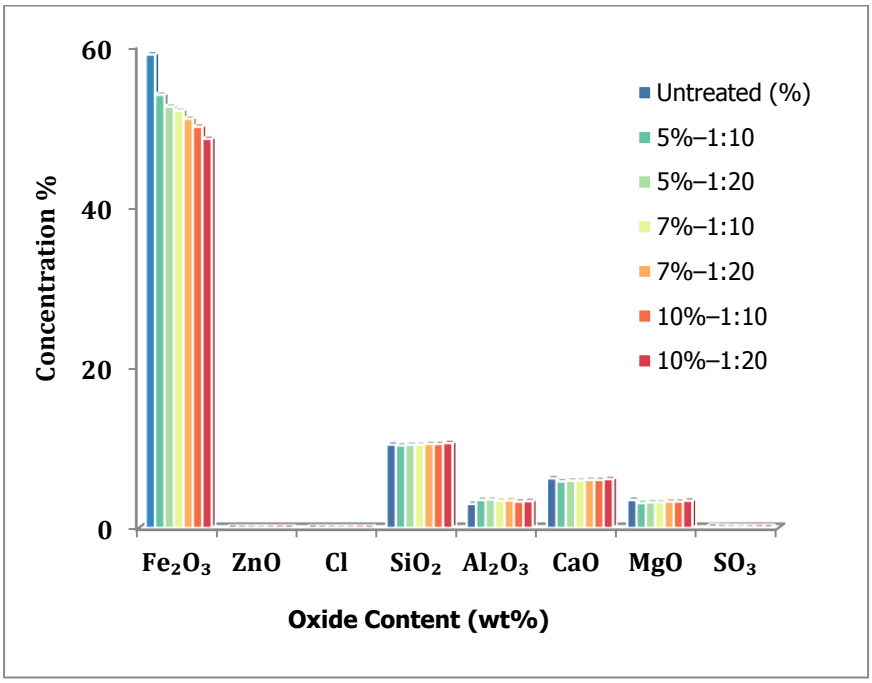

Figure 5: Effect of $NaNO_3$ treatment on black powder composition.

3.4. Comparison of $ZnCl_2$ and $NaNO_3$ Treatments

The results point to some clear differences between the two chemicals. Both $ZnCl_2$ and $NaNO_3$ reduced Fe_2O_3, but $ZnCl_2$ was noticeably stronger. In our case, the Fe_2O_3 content dropped to about 40.2 wt% with $ZnCl_2$, compared with around 48.5 wt% for $NaNO_3$. This makes sense, since chloride-rich acidic media usually have a higher capacity to dissolve iron oxides, which explains the stronger action of $ZnCl_2$. In $ZnCl_2$, Fe_2O_3 removal is promoted through protonation and chloride complexation (20), whereas $NaNO_3$ relies mainly on oxidative pathways (29), which are less aggressive. One major distinction between the two treatments is the formation of secondary residues. $ZnCl_2$ treatment resulted in a substantial increase in ZnO (up to ~16.8 wt%) and in chlorine (5–8.6 wt%), both of which originate from the salt itself. By contrast, $NaNO_3$ did not introduce Zn or Cl, but it did lead to an increase in Na_2O (1.3–1.8 wt%), indicating sodium retention from the solution. Other oxides showed more stable behavior. SiO_2 and CaO levels remained largely unchanged under both treatments, confirming their inertness in these conditions. Al_2O_3, however, rose significantly in $ZnCl_2$-treated samples but stayed nearly constant after $NaNO_3$ exposure. Smaller fluctuations were observed for MgO, K_2O, and various trace oxides in both cases, most likely due to surface redistribution rather than bulk chemical changes. At the end, $ZnCl_2$ acts more aggressively, removing Fe_2O_3 more efficiently, but it also leaves chloride and zinc residues behind. $NaNO_3$, on the other hand, works in a gentler way. Its effect is weaker, yet the residue is cleaner, with sodium as the main byproduct.

4. Conclusion

1. Both chemical treatments were effective in reducing iron oxide (Fe2O3), but ZnCl2 proved to be more effective. Fe2O3's concentration decreased from 59.0% to 40.2% (~32% reduction) by ZnCl2 due to dissolution and chloride complexation, while NaNO3's reduction was slightly lower at 48.5%.
2. A trade-off exists between treatment efficacy and secondary residues. ZnCl2's efficiency was offset by the introduction of zinc oxide (ZnO up to 16.8%) and chlorine (Cl up to ~8.6%), whereas $NaNO_3$ treatment, though less effective, was cleaner, introducing only sodium oxide (Na2O up to 1.8%).

3. Inert oxides remained essentially unchanged. SiO2 and CaO were stable in both treatments. Al2O3 increased notably under $ZnCl_2$ treatment but remained stable with $NaNO_3$. Other minor oxides (MgO, K_2 O, TiO_2 , MnO, P_2 O_5 , BaO) showed only small fluctuations, consistent with their lower reactivity.
4. Implications for pipeline maintenance. This study shows that chemical treatments can reshape the composition of black powder deposits once they have formed. $ZnCl_2$ works well when strong cleaning is needed, though the residues it leaves behind—mainly zinc and chloride—must be managed carefully. $NaNO_3$, on the other hand, provides a cleaner outcome but is less forceful in removing iron oxides. In practice, the choice between the two depends on what the operator values more: speed and strength of cleaning, or residue control and simplicity. Further testing under real pipeline conditions will be important to refine these methods and weigh their efficiency against environmental impact and cost.

References

[1] U.S. Energy Information Administration (EIA), "EIA projects nearly 50% increase in world energy usage by 2050, led by growth in Asia," *Today in Energy*, 2019. https://www.eia.gov/todayinenergy/detail.php?id=41433.

[2] A. Neacșa, C. N. Eparu, C. Panaitescu, D. B. Stoica, B. Ionete, A. Prundurel, and S. Gal, "Hydrogen–Natural Gas Mix—A Viable Perspective for Environment and Society," *Energies*, vol. 16, no. 15, p. 5751, 2023. DOI: 10.3390/en16155751.

[3] International Energy Agency, Gas Market Report – Q2 2024. https://www.iea.org/reports/gas-market-report-q2-2024.

[4] U.S. Energy Information Administration, International Energy Outlook 2023. https://www.eia.gov/outlooks/ieo/.

[5] J. Li, Y. She, Y. Gao, M. Li, G. Yang, and Y. Shi, "Natural gas industry in China: Development situation and prospect," Natural Gas Industry B, vol. 7, no. 6, pp. 604–613, 2020. DOI: 10.1016/j.ngib.2020.04.003.

[6] M. Debouza, A. Al-Durra, K. Al-Wahedi, and M. Abou-Khousa, "Assessment of black powder concentrations in natural gas pipeline networks," IEEE Access, vol. 8, pp. 71395–71404, 2020. DOI: 10.1109/ACCESS.2020.2987109.

[7] F. Esmaeilzadeh, D. Mowla, and M. Asemani, "Mathematical modeling and simulation of pigging operation in gas and liquid pipelines," *J. Petroleum Sci*. Eng., vol. 59, no. 3–4, pp. 210–218, 2007. DOI: 10.1016/j.petrol.2007.04.005.

[8] J. Nagaraj, "Smart pigging in high pressure gas pipeline: Practical problems and solutions—a case study," *in Proc. Pipeline Pigging and Integrity Management Conf*., Houston, TX, 2015. https://doi.org/10.1115/IOGPC2013-9826.

[9] H. Zhang, Q. Zheng, D. Yu, N. Lu, and S. Zhang, "Numerical simulation of black powder removal process in natural gas pipeline based on jetting pig," *J. Natural Gas Sci. Eng*., vol. 81, p. 103451, 2020. https://doi.org/10.1016/j.jngse.2018.07.022.

[10] Z. Belarbi, B. George, N. Moradighadi, D. Young, S. Nesic, M. Singer, and R. P. Nogueira, "Volatile corrosion inhibitor for prevention of black powder in sales gas pipelines," *in CORROSION*, pp. 1–16, 2018. DOI:10.5006/C2018-10962.

[11] F. S. Al Wahedi, M. H. Saleh, and Z. E. Dadach, "Black powder in sales gas pipelines: sources and technical recommendations," *World J. Eng. Techno*, vol. 8, no. 1, p. 60, 2020. DOI: 10.4236/wjet.2020.81007.

[12] M. F. Al Abri, H. Al Hosni, A. M. Al Rashdi, and S. M. Al Jibouri, "Geochemical characterization of black powder deposits in gas pipelines using sequential extraction and XRD/XRF analysis," *J. Natural Gas Sci. Eng*., vol. 104, p. 104658, 2022. DOI: 10.1016/j.jngse.2022.104658.

[13] A. Tessier, P. G. C. Campbell, and M. Bisson, "Sequential extraction procedure for the speciation of particulate trace metals," *Anal. Chem*., vol. 51, no. 7, pp. 844–851, 1979.

[14] X. Qi, Z. Wei, Y. Wang, M. Liu, M. Tian, and Y. Liu, "Surface treatment of reduced iron powder with amino trimethylene phosphonic acid and inorganic synergists for high saturation magnetization and low-loss soft magnetic composites," *Mater. Chem*., 2025. https://doi.org/10.1016/j.matchemphys.2025.130661

[15] M. Sandhya, D. Ramasamy, K. Sudhakar, K. Kadirgama, and W. S. W. Harun, "Ultrasonication an intensifying tool for preparation of stable nanofluids and study the time influence on distinct properties of graphene nanofluids–A systematic overview," *Ultrasonics*, 2021. https://doi.org/10.1016/j.ultsonch.2021.105479.

[16] M. Colahan, D. Young, M. Singer, and R. P. Nogueira, "Black powder formation by dewing and hygroscopic corrosion processes," *J. Natural Gas Sci. Eng.*, vol. 56, pp. 358–367, 2018. https://doi.org/10.1016/j.jngse.2018.06.021.

[17] Khuraibut, Yousef. "Study on Elemental Sulfur Formation from Black Powder Deposits." *In AMPP CORROSION*, p. D031S029R014. AMPP, 2022.

[18] M. Y. Wang, H. Y. Yao, Y. F. Liu, Y. S. Zhu, W. B. Chen, Y. Z. Xu, and Y. Huang, "Understanding and probing progression of localized corrosion on inner walls of steel pipelines: an overview," *J. Iron Steel Res. Int.*, vol. 32, 2025. https://doi.org/10.1007/s42243-024-01213-6.

[19] J. S. Smart, "Black powder in gas pipelines," *in Texas Gas Association Conf.*, Nov. 2014.

[20] D. Nakhaie and E. Asselin, "The dissolution kinetics and salt film precipitation of Zn and Fe in chloride solutions: Importance of the common-ion effect and diffusivity," *Corros. Sci.*, vol. 149, pp. 108–121, 2018. https://doi.org/10.1016/j.corsci.2018.10.024.

[21] X. Chen, B. Bayanheshig, Q. Jiao, X. Tan, and W. Wang, "Numerical simulation of ultrasonic enhancement by acoustic streaming and thermal effect on mass transfer through a new computation model," *Int. J. Heat Mass Transfer*, vol. 171, 2021. https://doi.org/10.1016/j.ijheatmasstransfer.2021.121074.

[22] S. Rajan et al., "Synthesis of ZnO nanoparticles by precipitation method: characterizations and applications in decipherment of latent fingerprints," *Mater. Today: Proc.*, 2023. https://doi.org/10.1016/j.matpr.2023.05.680.

[23] A. G. Vega-Poot, G. Rodríguez-Gattorno, O. E. Soberanis-Domínguez, R. T. Patiño-Díaz, M. Espinosa-Pesqueira, and G. Oskam, "The nucleation kinetics of ZnO nanoparticles from $ZnCl_2$ in ethanol solutions," Nanoscale, vol. 2, no. 12, pp. 2710–2717, 2010. https://pubs.rsc.org/en/content/articlelanding/2010/nr/c0nr00439a.

[24] J. Lee, E. J. Jang, and J. H. Kwak, "Acid-base properties of Al_2O_3 : Effects of morphology, crystalline phase, and additives," *J. Catal.*, vol. 345, pp. 135–148, 2017. https://doi.org/10.1016/j.jcat.2016.11.025.

[25] Z. Bi, K. Li, C. Jiang, J. Zhang, S. Ma, M. Sun, Z. Wang, and H. Li, "Performance and transition mechanism from acidity to basicity of amphoteric oxides (Al_2O_3 and B_2O_3) in SiO_2 -CaO-Al_2O_3 -B_2O_3 system: A molecular dynamics study," *Ceram. Int.*, 2021. https://doi.org/10.1016/j.ceramint.2021.01.074.

[26] R. J. Robertson and A. S. Kucharski, "Thermodynamic properties of zinc chloride in alkali chloride melts by electromotive force measurements," *Can. J. Chem.*, vol. 51, no. 18, pp. 3114–3122, 1973. DOI: 10.1139/v73-466.

[27] F. Locati, S. Marfil, E. Baldo, and P. Maiza, "Na_2O, K_2O, SiO_2 and Al_2O_3 release from potassic and calcic-sodic feldspars into alkaline solutions," *Cem. Concr. Res.*, vol. 40, no. 8, pp. 1189–1196, 2010. https://doi.org/10.1016/j.cemconres.2010.04.005.

[28] H. Hu, X. Li, X. Gao, L. Wang, B. Li, F. Zhan, Y. He, L. Qin, and X. Liang, "A review on the multifaceted effects of δ-MnO_2 on heavy metals, organic matter, and other soil components," *RSC Adv.*, vol. 14, pp. 37752–37762, 2024. https://doi.org/10.1039/d4ra06005a.

[29] E. V. Bogorodskii, S. G. Rybkin, and V. G. Barankevich, "Kinetics of the interaction of iron, copper, and nickel sulfides with a sodium nitrate–sodium carbonate mixture," *Russ. J. Inorg. Chem.*, vol. 56, no. 6, pp. 831–834, 2011.